Environmental Science and Pollution Research (2022) 29:53225–53237
https://doi.org/10.1007/s11356-022-19606-z

RESEARCH ARTICLE

Rational design of Ag_2CO_3-loaded SGO heterostructure with enhanced photocatalytic abatement of organic pollutants under visible light irradiation

Neenamol John[1] · Ragam N. Priyanka[1] · Thomas Abraham[1] · Mamatha Susan Punnoose[1] · Bony K. John[1] · Beena Mathew[1]

Received: 21 September 2021 / Accepted: 3 March 2022 / Published online: 12 March 2022

Abstract

The photocatalytic activity of semiconducting silver carbonate was restricted by the lower stability and fast recombination rate of photogenerated electron–hole pairs. Sulfur-doped graphene oxide (SGO) is used as a cocatalyst for improving the photocatalytic activity of Ag_2CO_3 by reducing the recombination rate. A simple precipitation method was used for the modification of silver carbonate. The chemical, physical, optical, and electrochemical properties of the modified photocatalyst was characterized by XRD, SEM, TEM, UV–vis DRS, XPS, CV, impedance, and amperometry. The fabricated SGO-Ag_2CO_3 composite was successfully degraded various organic pollutants such as methylene blue (MB), rhodamine B(RhB), methyl orange (MO), tartrazine, and thiram with augmented mineralization. The optimization of weight percentage of the developed binary composite with 0.5% SGO-Ag_2CO_3 showed enhanced photocatalytic degradation and followed pseudo-first-order kinetics with rate constant 0.126. More than 90% of degradation efficiency of the pollutants within a short time promises the binary heterostructure for future industrial applications. The excellent stability and reproducibility of the composite opened a new route in the treatment of wastewater.

Keywords Sulfur-doped graphene oxide · Silver carbonate · Organic dyes · Thiram

Introduction

The effect of wastewater pollution is a major environmental apprehension on both the environment and humans. Discharge of organic pollutants directly into the environment by different forms which affect animals and human beings (Arunpandian et al. 2019). Nowadays, industrial and agricultural effluents are referred to as the major group of contaminants. Organic dyes and pesticides are the pollutants of our water systems. There are lots of conventional methods like flocculation, coagulation, biodegradation, and adsorption are available for wastewater purification (Khurram et al. 2021). The major disadvantage of these methods is only just a shift of contaminants from one system to another, and there is no complete removal or degradation of pollutants (Hunge et al. 2018). So researchers tried to develop an advanced green method for environmental remediation.

Photocatalysis is a green and energy saving strategy in the field of environmental cleaning (Dong et al. 2017). In the photocatalytic process, there is a chance for utilizing a wide range of natural sunlight for the removal of organic pollutants like organic dyes and pesticides without any formation of harmful by-products. Carbon dioxide and water are the major degraded products of this process (Liu et al. 2018). Fabrication of a good photocatalyst is one of the challenging tasks of this field. Absorption of a wide range of sunlight, efficient charge separation and transfer, strong redox ability, excellent recyclability, and great stability are the characteristics of a good photocatalyst (Liu et al. 2019). Semiconducting metal oxide like TiO_2 (Low et al 2018; Safajou et al. 2017), ZnO (Pirhashemi and Habibi-Yangjeh 2018; Li et al. 2017) are conventionally used photocatalysts, but the major drawback of this type of catalysts is the wide band gap energy that will decrease the photocatalytic efficiency (Liu et al. 2021). Over the

Responsible editor: Sami Rtimi

✉ Beena Mathew
beenamathew@mgu.ac.in

[1] School of Chemical Sciences, Mahatma Gandhi University, Kottayam 686560, Kerala, India

last few years, Ag-containing compounds have been used as photocatalysts due to its excellent photoresponse (Xu et al. 2015a, b). Silver-based materials indicate advantages as photocatalyst due to the significant SPR effect of silver nanoparticles that are formed on their surface (Asadollahi et al. 2017). Recently reported silver-based photocatalysts are Ag_2O (Chen et al. 2018), AgX (X = Cl, Br, I) (Han et al. 2013), Ag_2CrO_4 (Xu et al. 2015a, b), Ag_3PO_4 (Yi et al. 2010), Ag_3VO_4 (Wang et al. 2014a, b, c), Ag_2WO_4 (Longo et al. 2013), Ag_3AsO_4 (Tang et al. 2013), $Ag_8W_4O_{16}$ (Wang et al. 2014a, b, c), $AgInW_2O_8$ (Hu et al. 2010), $Ag_2Mo_3O_{11}$ (Feng et al. 2011), $AgNbO_3$ (Wang et al. 2013), $AgSbO_3$ (Liu et al. 2012), and Ag_2CO_3 (Dai et al. 2012; Zhu et al. 2016). However, poor stability is one of the disadvantages of silver-based semiconducting nanomaterials. The reduction of Ag^+ ion to Ag(0) is the reason for the unstability of silver compounds. So it is obligatory to transfer the photogenerated electrons from the surface of silver compounds to an acceptor material to enhance stability and photocatalytic activity (Priyanka et al. 2020).

Silver carbonate is a semiconducting light sensitive material with a narrow band gap (2.30 eV) (Wu et al. 2019; Xie et al. 2016), but this is very sensitive to light that will lead to poor stability. Formation of metallic silver (Ag(0)) under light irradiation is the reason for the poor stability of silver carbonate (Wang et al. 2017). In order to overcome this drawback of silver carbonate, there are lot of methods like hybridization, modification, morphology, and size control are used (Wu et al. 2019; Liu et al. 2019). Among these methods modification of photocatalyst with other nanomaterials was generally used strategy for the photocatalytic property improvement. The development of nanocomposite will help to overcome the stability problem of silver carbonate. Silver carbonate was modified using materials like ZnO (Li et al. 2019), TiO_2 (Wang et al. 2014a, b, c), CeO_2 (Wen et al. 2018), AgX (X = Cl, I) (Dostanić et al. 2017), MoS_2 (Fu et al. 2019), $LaFeO_3$ (Pirzada et al. 2019), AgBr (Arumugam Senthil et al. 2020), BiO_2CO_3 (Li et al. 2016), N-doped graphene (Song et al. 2017), and g-C_3N_3 (Li et al. 2015). All these silvercarbonate nanocomposites are applicable for different organic pollutant removals from wastewater.

Carbon-based materials are often used to reform the catalyst; graphene oxides, graphene sheets, carbon nanotubes, and activated carbon are commonly used carbon materials for the modification of photocatalyst (Zhu et al. 2016). This carbonatious material is again modified with heteroatoms like sulfur, boron, and nitrogen. For photocatalytic application, sulfur doping is an efficient method for pollutant removal from wastewater. Sulfur-doped carbon materials are widely used for different applications like catalytic ozonation, hydrogen generation, oxygen, and reduction reactions (ORR). Compared to carbon, sulfur has more valence electrons; those additional electrons are transferred to carbon, which will change the electronic properties of carbon material (Priyanka et al. 2020).

In this work sulfur-doped graphene oxide is used as a cocatalyst for improving the photocatalytic activity of silver carbonate. The SGO-Ag_2CO_3 nanocomposite was synthesized by a simple precipitation method. The physical, chemical, optical, and electrochemical properties are studied using different characterization techniques. The highlight of the work is the effective treatment of various refractory pollutants such as dyes and pesticides using sunlight irradiation. The catalyst was found as stable and recyclable up to four cycles, and the organic pollutants were well mineralized within the short time period.

Experimental

Materials

Silver nitrate ($AgNO_3$), sodium carbonate (Na_2CO_3), graphite powder, sodium sulfide (Na_2S), and hydrazine hydrate ($H_2NNH_2{\cdot}H_2O$) used were of analytical grade. Methylene blue, rhodamine B, methyl orange, and tartrazine were purchased from Merck, India, and were used without purification. Fungicide dithiocarbamate (thiram) was purchased from Sigma-Aldrich.

Synthesis of photocatalysts

Synthesis of SGO

Modified Hummers method was used for the synthesis of GO (Xu et al. 2015a, b), simple microwave irradiation technique was required for the synthesis of sulfur-doped graphene oxide. 0.05 g of GO was dispersed in deionized water (100 mL) and sonicated for 30 min. Na_2S (0.5 M) was added and again sonicated for 30 min. After sonication, the GO-Na_2S mixture undergoes microwave irradiation (800 W) for 15 min. The synthesized SGO was washed with deionized water and dried at 80°(Priyanka et al. 2020).

Synthesis of SGO-Ag_2CO_3

Different weight percentage of SGO (0.4, 0.5, 0.6%) were dispersed in 15 mL of 0.1 M silver nitrate solution. The mixture was sonicated for 30 min, and 0.1 M sodium carbonate (5 mL) was added slowly. The mixture was kept for 20 min with stirring. The green-yellow precipitate was washed and dried at 60 °C to get SGO-Ag_2CO_3 (Scheme 1).

Scheme 1 Synthesis of SGO-Ag_2CO_3

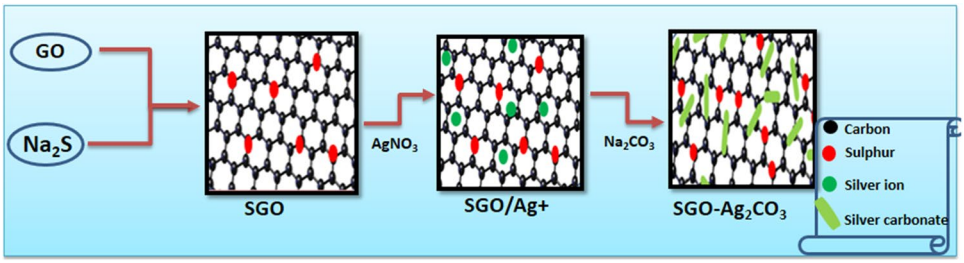

Charaterizations

The various SGO-Ag_2CO_3 nanocomposites were characterized using different analytical, spectroscopic, and electrochemical techniques. Fourier transform infrared (FT-IR) spectroscopy was carried out for analyzing functional group and bonding between the elements using Perkin Elmer 400 spectrometer with wavenumber ranges from 4000 to 400 cm^{-1}. X-ray diffraction (XRD) studies were carried out using Bruker AXS D8 Advance X-ray diffractometer with Cu Kα radiation (λ = 1.5406 A°). The band gap and absorbance of the synthesized semiconducting material were studied using UV–vis DRS analysis (Shimadzu UV-3600 Plus, Japan). The photoluminescence (PL) spectra of the nanocomposites were analyzed by the Shimadzu RF-6000 spectrofluorometer. The morphology of the modified photocatalyst was studied using scanning electron microscopy (JEOL-JSM-6390) and transmission electron microscopy (JEOL JEM-2100 microscope). The elemental composition of the nanocomposite was studied by EDX analysis. X-ray photoelectron spectra (XPS) were carried out using a VG Multi-Lab 2000 system with a monochromatic Mg Kα source at 20 kV to find out the chemical states of the nanocomposite. The degradation of the pollutants was confirmed using TOC (TOCVCPH Total Carbon Analyzer, Shimadzu Corporation, Japan) and HPLC (SPD-20A, Shimadzu Corporation, Japan) analysis. The electrochemical analysis of the composite was studied using Biologic SP-200 model electrochemical workstation. The three electrodes electrochemical cell with glassy carbon electrode (GCE), platinum wire, and Ag/AgCl were used as working, counter, and reference electrodes, respectively.

Photocatalytic study

For the photodegradation experiment, about 0.025 g of the catalyst was taken in a 100 mL beaker and 50 mL of dye solution (10 mg/L); thiram (20 mg/L) was added. The mixture was sonicated for 15 min and further stirred for 45 min in the dark reaching adsorption–desorption equilibrium. About 2 ml of the catalyst containing dye solution was taken, centrifuged, and then labeled as dark. The bulk catalyst-dye mixture was subjected to sunlight irradiation, and in each 30 min time interval, 2 mL solution was withdrawn centrifuged and labeled. A Shimadzu UV-2450 spectrophotometer was used to measure the change in absorbance of dye solution after irradiation of sunlight. The studies were carried out in the month of November to December at 11 am to 1 pm. The degradation efficiency of the photocatalyst was measured by using the following equation.

$$\text{Degradationefficiency}(\%) = (C_0 - C_t)/C_0 \times 100 \quad (1)$$

where C_o is the initial concentration of the MB and C_t is the concentration of the MB after t min of sunlight irradiation.

The active species of the photocatalytic system were identified by a scavenger study. In this experiment, 1 mM of a reagent such as 1,4-benzoquinone (1,4-BQ) was used as superoxide (O_2^-) radical scavenger, a disodium salt of ethylenediaminetetraacetic acid (EDTA) was used as hole (h^+) scavenger, isopropyl alcohol (IPA) was used as hydroxyl (•OH) radical scavenger. The photodegradation was carried out as aforementioned.

Results and discussion

Crystal structure and bonding

The crystal structure of the synthesized product was studied by XRD. Figure 1a represent XRD pattern of Ag_2CO_3, SGO, and different weight percentage (0.4, 0.5, 0.6%) of SGO-Ag_2CO_3 crystal. The inset of Fig. 1a shows the XRD peak of SGO where the peak corresponds to the (002) plane 20°–30° range (Han et al. 2018). All the diffraction peaks can be well-indexed to a monoclinic phase of silver carbonate (JCPDS No: 12–766) (Petala et al. 2020). The XRD peaks of SGO-Ag_2CO_3 composites were analogous to those of pure Ag_2CO_3. There is no extra peak observed for SGO due to its low weight percentage. The sharp XRD peaks indicate the high crystalline nature of the nanocomposite. The presence of the functional groups involved in the nanocomposite can be identified using FT-IR analysis (Fig. 1b). The spectrum of SGO (SI: 1) shows peaks at 1200 and 1500 cm^{-1} corresponding to C-S bonds (Priyanka et al. 2020), while the

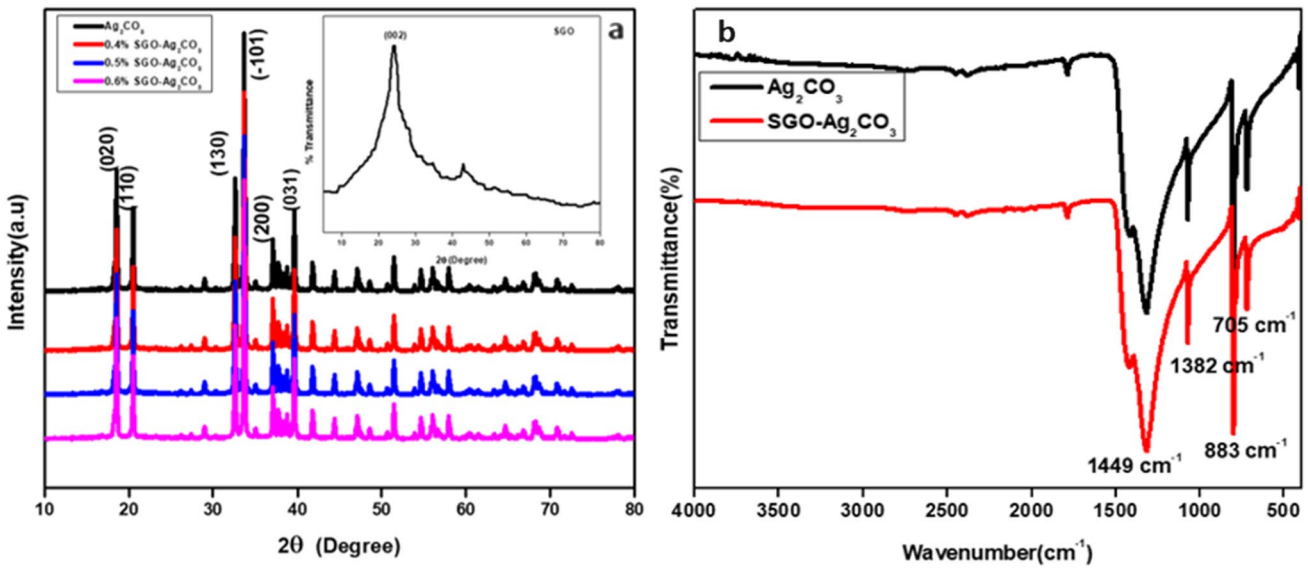

Fig. 1 **a** XRD spectra of Ag_2CO_3, SGO, and 0.4, 0.5, 0.6 wt% of SGO-Ag_2CO_3, and **b** FT-IR spectra of Ag_2CO_3 and 0.5% SGO-Ag_2CO_3

peak at 1738 cm^{-1} corresponds to the presence of C = O bond. In the FT-IR spectra of the pure Ag_2CO_3 and SGO-Ag_2CO_3 composites, the characteristic absorption bands of CO_3^{-2} could be observed at 705, 883, 1382, and 1449 cm^{-1}. Due to the presence of SGO in the chemical environment of the pure silver carbonate, there is a small difference in the peak intensity of the SGO-Ag_2CO_3 (0.5 wt %) composite (Xu et al. 2014). As expected, the FT-IR spectrum of 0.5% SGO modified Ag_2CO_3 demonstrates the presence of the peaks from both SGO and Ag_2CO_3 with minor shift confirming the formation of the composite (Wen et al. 2018; Yu et al. 2016; Tonda et al. 2015).

UV–vis DRS analysis

The absorption region of the semiconducting photocatalyst was identified with the help of UV–vis. spectroscopy. Figure 2 shows the absorption spectra and Tauc plot of Ag_2CO_3, SGO 0.4, 0.5, and 0.6% SGO-Ag_2CO_3. The absorption of 0.5% SGO-Ag_2CO_3 is higher than pristine Ag_2CO_3. From the absorption spectra, the band gap of

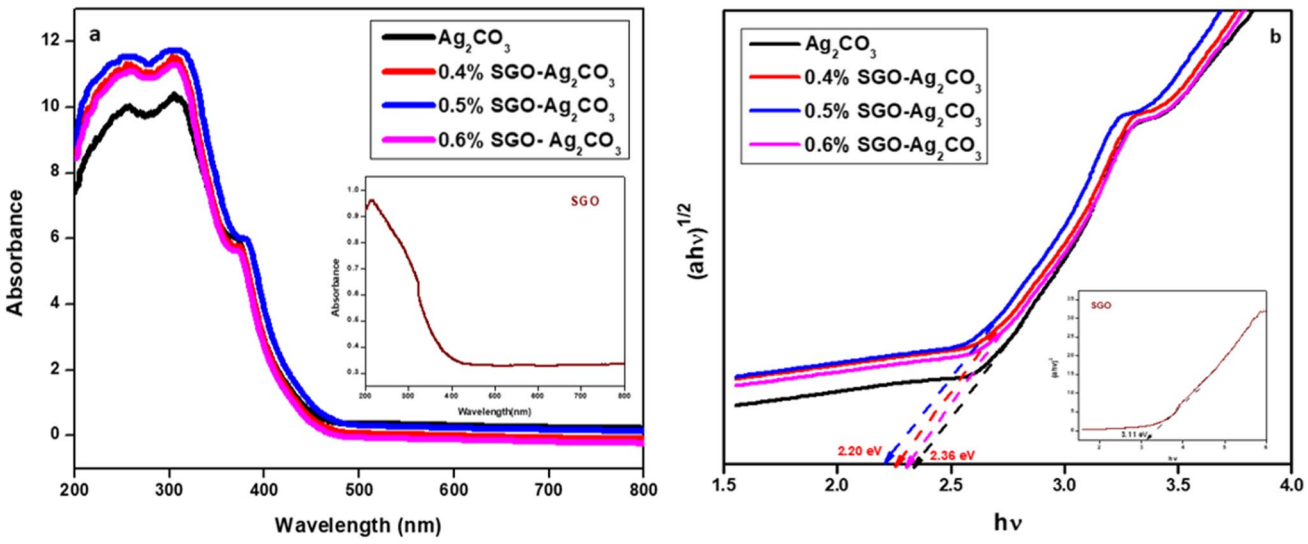

Fig. 2 **a** UV–vis DRS spectra of Ag_2CO_3, SGO, and 0.4, 0.5, 0.6 wt% SGO-Ag_2CO_3 and **b** Tauc plot of Ag_2CO_3, SGO and 0.4, 0.5, and 0.6 wt % SGO-Ag_2CO_3

the synthesized photocatalyst can be calculated using the equation:

$$\alpha h\upsilon = A(h\upsilon - Eg)^n \quad (2)$$

where α, h, υ, A, Eg, and n are the absorption coefficient, Planck's constant, light frequency, proportionality constant, and band gap. The value n depends upon the nature of the semiconductor, for indirect transition $n = 2$ and for direct transition $n = 1/2$. The value of Eg and n were determined using the plot of ln (ahυ) versus ln (hυ – Eg).The following equations are used to determine the potential of the valence band (VB) and conduction band (CB):

$$E_{VB} = X - Ee + 0.5Eg \quad (3)$$

$$E_{CB} = E_{VB} - Eg \quad (4)$$

where E_{VB} is the valence band potential, X is the electronegativity of the semiconductor, Ee is the energy of free electron on the hydrogen scale, and Eg is the calculated band gap of the semiconducting material (Xu et al. 2011). Using Eqs. (3) and (4), the E_{VB} calculated for Ag_2CO_3 is 2.70 eV, and E_{CB} is 0.34 eV. After modification with SGO, the band gap of silver carbonate was reduced from 2.36 to 2.20 eV that will enhance the transfer of electron from valence band to conduction band.

Photoluminescence spectra

The effect of charge carrier recombination rate and the semiconducting behavior of SGO-Ag_2CO_3 in the visible region can be easily explained by photoluminescence spectra. If the PL signal intensity is low, the electron–hole recombination rate is lower. It indicates a longer lifetime of the charge carriers such as electrons and holes. The spectrum of PL intensity versus wavelength (450–600 nm) of the synthesized SGO-Ag_2CO_3 and Ag_2CO_3 is shown in Fig. 3. PL spectra of Ag_2CO_3 0.4, 0.5, and 0.6% SGO-Ag_2CO_3 composites illustrate that both pure Ag_2CO_3 and the modified Ag_2CO_3 possess the same pattern of emission but with a huge difference in intensity.

The PL signal intensity of SGO-Ag_2CO_3 is found much smaller than Ag_2CO_3, which means recombination of photo-induced charge carriers is decreased in SGO-Ag_2CO_3 than Ag_2CO_3. This reduction of recombination will enhance the photocatalytic activity of this synthesized photocatalyst since the carriers are more available to react with O_2 or H_2O in the photocatalytic system to produce active radical species like $^{\cdot}O_2^-$ and $^{\cdot}OH$ (Tian et al. 2016).

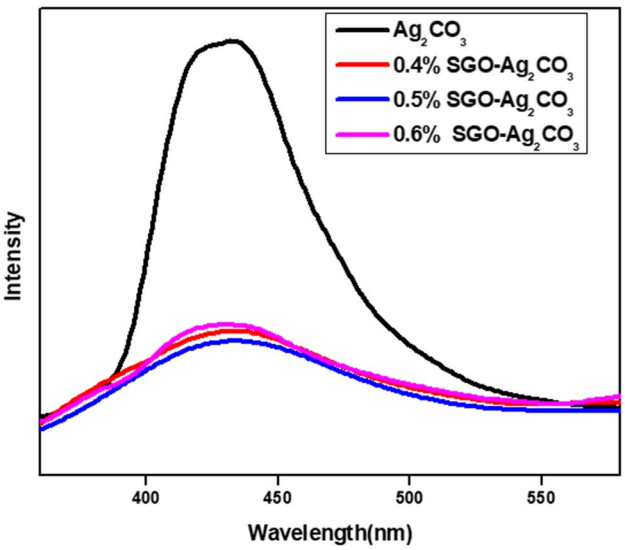

Fig. 3 PL spectra of Ag_2CO_3, 0.4, 0.5, and 0.6 wt% SGO-Ag_2CO_3

XPS analysis

The chemical state and composition of the developed composite were further determined using XPS analysis. XPS spectra of SGO-Ag_2CO_3 are shown in Fig. 4. XPS survey spectrum (Fig. 4a) is one of the evidence for the formation of pure photocatalyst because there involves the presence of only C, O, Ag, and S in the photocatalyst. This clearly identifies that the preparation process does not bring any impurities. The high-resolution XPS spectra of SGO-Ag_2CO_3 contain the peaks of carbon (C 1 s), oxygen (O 1 s), silver (Ag 3d), and sulfur (S 2p). The XPS spectrum of SGO-Ag_2CO_3 is almost similar to the spectrum of pure silver carbonate (SI: 2) except the presence of peaks of sulfur. The C = C bond of SGO (Priyanka et al. 2020) and carbonate ion of Ag_2CO_3 (Yu et al. 2016) of SGO-Ag_2CO_3 composite are observed at 286.043 and 281.954 eV, respectively (Fig. 4b). The Fig. 4c indicates that the O 1 s position is around 528 eV and that peak represents O^{2-} in SGO-Ag_2CO_3. In pure silver carbonate, the XPS of Ag 3d showed a double peak at 374.1 (Ag $3d_{3/2}$) and 368.1 eV (Ag $3d_{5/2}$). However, in the case of SGO-Ag_2CO_3, the peak of Ag 3d had a minor shift about 3 eV (Fig. 4d). The high intense peaks represent Ag(+) state of silver carbonate and the less intense peak corresponds to Ag(0) state of AgNPs. The interaction between SGO and silver carbonate will affect the factors such as electronegativity, lattice potential, and extra-atomic relaxation energy and result in a slight shift (Fu et al. 2019; Priyanka et al. 2021). As the modified nanocomposite contains only 0.5% of SGO. Hence the S 2p is not obtained as a clear peak like other elements. The peaks around 166 and 170 eV indicate the C–S–C and C–SOx–C bonds in SGO, respectively (Tian et al. 2016). The formation of the binary

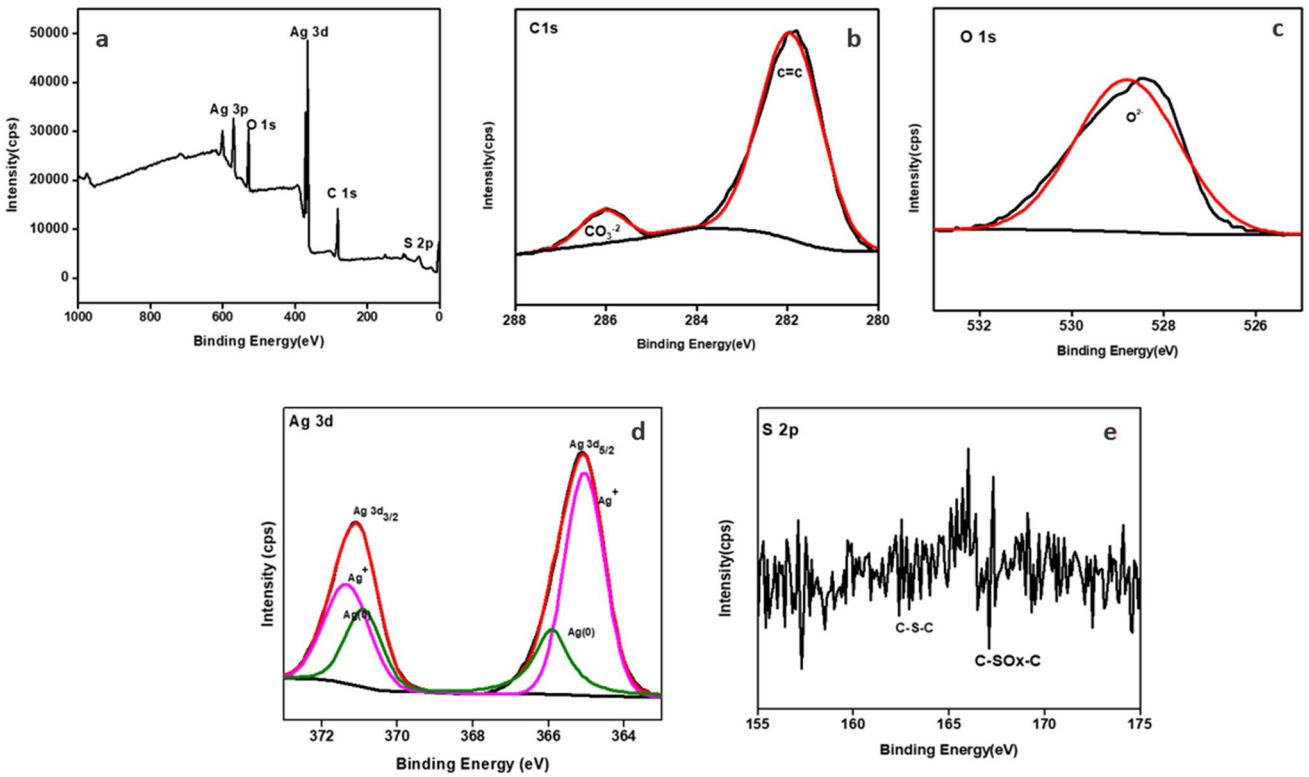

Fig. 4 **a** XPS survey spectrum of SGO-Ag_2CO_3 and high-resolution XPS spectra of **b** C 1 s, **c** O 1 s, **d** Ag 3d, **e** S 2p

heterojunction SGO-Ag_2CO_3 photocatalyst is confirmed with the XPS analysis results.

Morphology studies

The surface morphology of the synthesized composite was studied by scanning electron microscopy. Figure 5(a, b) displays the SEM images of silver carbonate and 0.5% SGO-Ag_2CO_3. The sharp identification of the presence of small rods reveals the formation of nanomaterial. The figure clearly shows the presence of SGO as sheets above which the Ag_2CO_3 rods are sporadically distributed. The mean length of silver carbonate nanorod is about 762 nm. There is a synergetic interaction between SGO and Ag_2CO_3. This morphology allows the transfer of charge carriers between the SGO sheets and the embedded Ag_2CO_3 rods on it, which is a favorable morphology for an efficient photocatalyst.

The inner morphological aspects of the developed composite can be analyzed using transmission electron microscopy (TEM). Figure 6a and b show the TEM images of silver carbonate and SGO-Ag_2CO_3. As shown in the SEM image, the rod-shaped structure of Ag_2CO_3 was clearly depicted

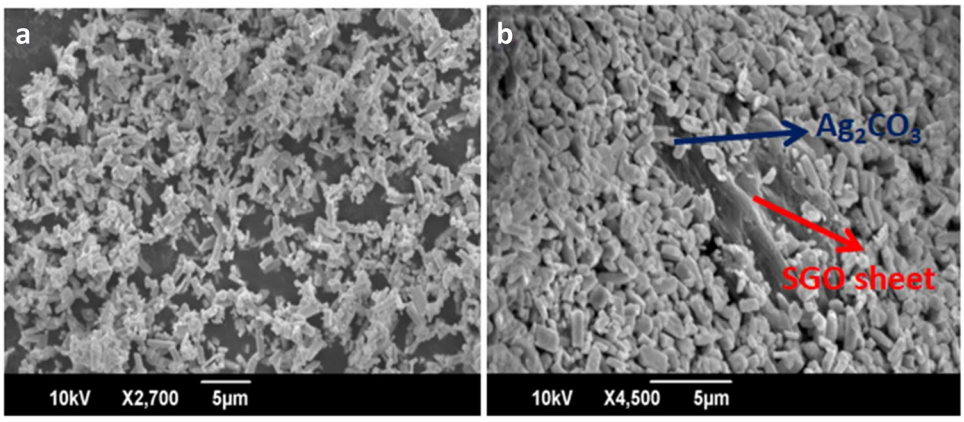

Fig. 5 SEM of **a** Ag_2CO_3 and **b** SGO-Ag_2CO_3

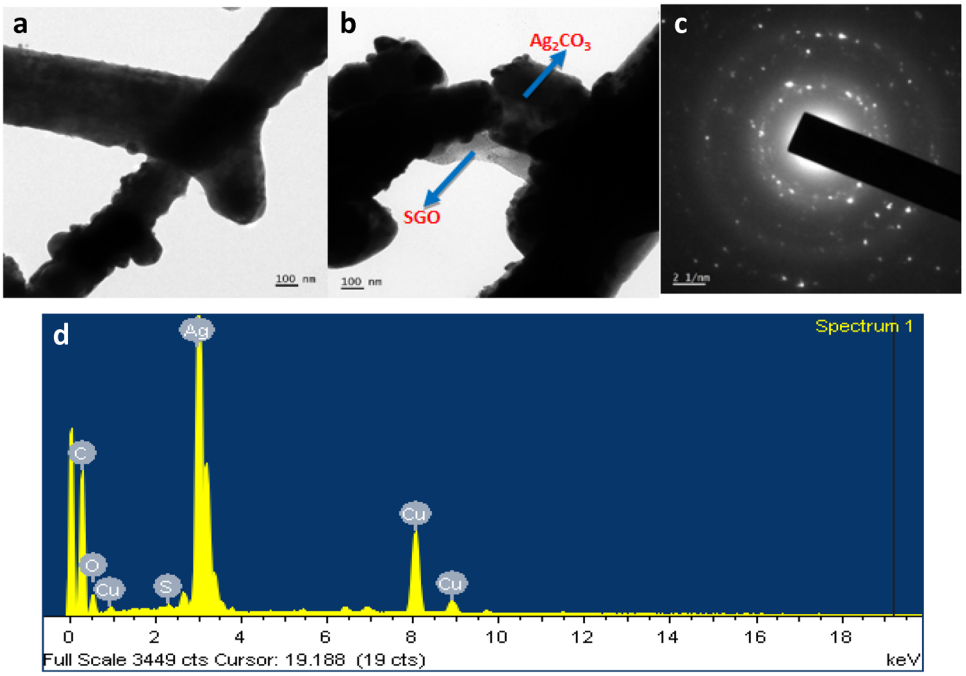

Fig. 6 TEM of **a** Ag_2CO_3, **b** SGO-Ag_2CO_3, **c** SAED pattern, and **d** EDAX spectrum of SGO-Ag_2CO_3

using TEM analysis. The short rod of silver carbonate distributed on the surface of SGO sheet can be visualized in the figure. The diameter of single rod is about 650 nm. The selected area electron diffraction (SAED) pattern of SGO-Ag_2CO_3 contains both rings and spots (Fig. 6c). The bright spot represents the crystalline nature, and different rings are due to the Braggs reflections from different planes. The presence of several rings is indicative of the poly crystalline nature of the composite. To account for the elemental composition, EDX analysis was carried out. This confirmed the presence of elements sulfur, carbon, oxygen, and silver in SGO-Ag_2CO_3 composite (Fig. 6d).

Electrochemical study

The conductivity of the synthesized nanocomposite was evaluated by electrochemical analysis. The response of photocatalyst towards current was studied using cyclic voltammetry (CV). Glassy carbon electrode (GCE) was used as a working electrode. For this SGO, Ag_2CO_3 and SGO-Ag_2CO_3 nanomaterials were coated on the surface of the working electrode. In the cyclic voltammetry study, the mixture of 5 mM$[Fe(CN)_6]^{3-}$/$[Fe(CN)_6]_4$ and 0.1 M KCl are used as electrolyte. From the cyclic voltammogram of these three nanomaterials, SGO has no redox peak, silver carbonate and SGO-Ag_2CO_3 showed the presence of redox peak, but the area of cyclic voltammogram are different. After modification with SGO, the area of cyclic voltammogram increased (Fig. 7a), and this indicates that doping with cocatalyst leads to the significant change of the activity of the silver carbonate. This is due to the enhanced charge mobility and availability of charged species which gives a positive impact for degradation of pollutants. Electrochemical impedance spectroscopy (EIS) was used to study the charge carrying capacity of nanomaterial. Generally, EIS analysis represents in the form of Nyquist plots by applying on working electrode (GCE) coated with nanomaterial. The Nyquist plots obtained for these materials were semicircular shapes with a tail at higher frequencies. The radius of this semicircle implies the effectiveness of charge transfer resistance (R_{ct}). The large radius of the semicircle denotes higher charge transfer resistance, low charge separation efficiency, and least charge flow. Similarly, the material with low semicircular radius of impedance spectra has low charge transfer resistance higher charge separation and flow. Here, the obtained Nyquist plots of SGO, Ag_2CO_3, 0.4, 0.5, and 0.6% SGO-Ag_2CO_3 are shown in Fig. 7b. The plot shows low resistance for the developed binary composite on comparing with the pure compounds suggesting the improved activity of the composite. The activity of nanophotocatalyst upon irradiation with light was studied using amperometry. The intensity of the photocurrent becomes improved after modification with SGO. In comparison with the unmodified silver carbonate, the enhanced for SGO-Ag_2CO_3 shows its excellent catalytic activity. The Xenon lamp (300 W) and 0.5 M Na_2SO_4 acted as a light source and electrolyte. When the nanocomposite was irradiated with light, the availability of charged species increased, which enhanced the photocurrent. Figure 7c shows photocurrent measurement of SGO, Ag_2CO_3, and SGO-Ag_2CO_3 (Abraham et al. 2020; Joseph et al. 2019).

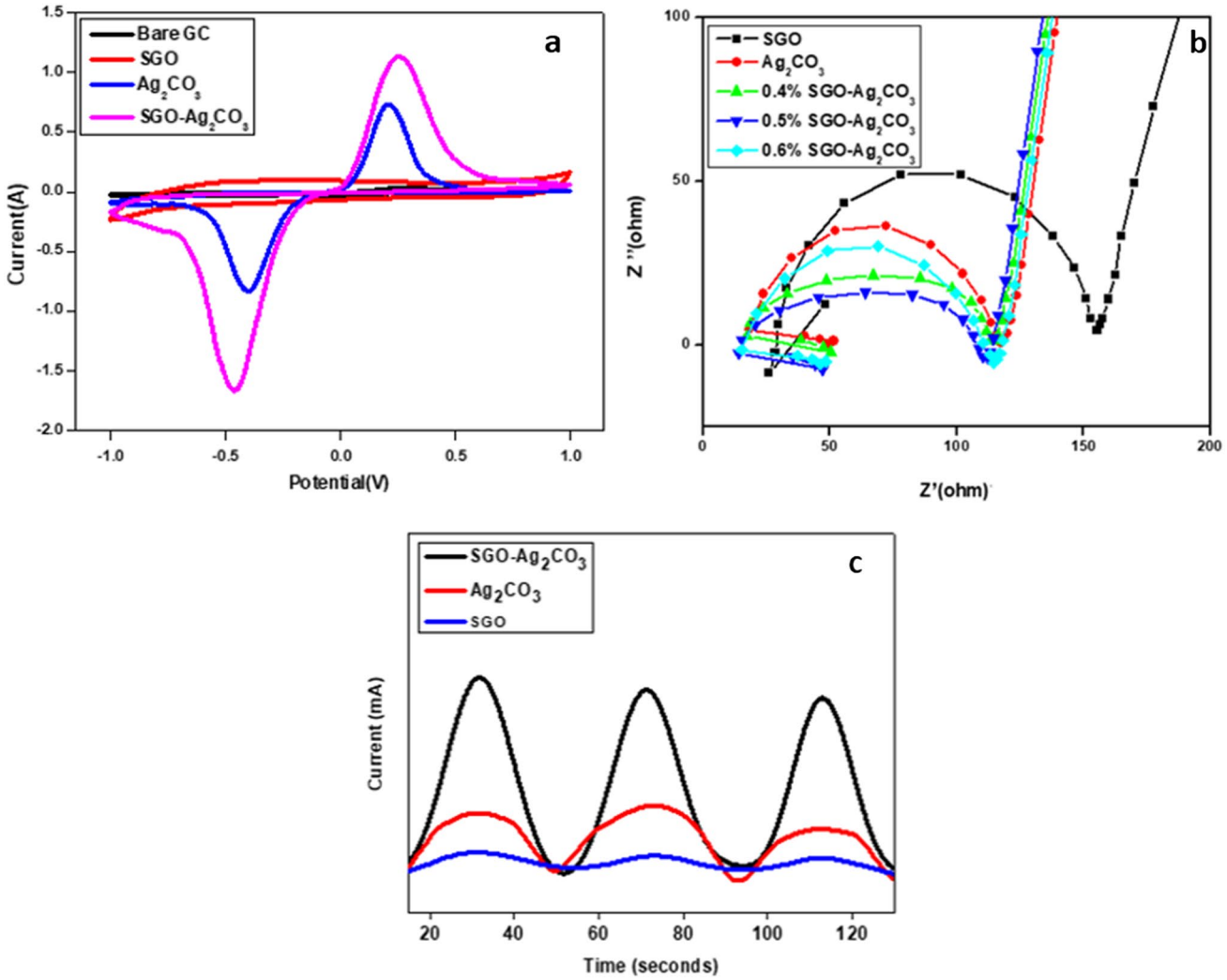

Fig. 7 **a** Cyclic voltammogram of bare GC, SGO, Ag_2CO_3, and SGO-Ag_2CO_3, **b** impedance spectra of SGO, Ag_2CO_3, 0.4, 0.5, and 0.6% SGO-Ag_2CO_3, and **c** amperometric study of and SGO, Ag_2CO_3, and SGO-Ag_2CO_3

Photocatalytic activity

The degradation ability of the SGO-Ag_2CO_3 composite was studied by taking one of the most prominent water pollutant organic dye methylene blue (MB) as the model compound. Figure 8 represents a comparison of photocatalytic activities of silver carbonate and SGO-Ag_2CO_3. After modification with SGO, the activity of silver carbonate increased. SI: 3 depicts the C/Co and –ln C/Co vs. time plot of Ag_2CO_3 and SGO-Ag_2CO_3. From the kinetic study, the photocatalytic degradation reaction is assumed to follow pseudo-first-order kinetics according to the equation:

$$-\ln C/Co = kt \quad (5)$$

where k and t are the rate constant and time, respectively (Priyanka et al. 2021). From the optimization study, it is observed that the extent of MB degradation is highest for the 0.5% composite with SGO than those with 0.4 and 0.6% SGO. Thus, it can be confirmed that 0.5% SGO-Ag_2CO_3 is a more efficient photocatalyst than 0.4 and 0.6% SGO-Ag_2CO_3 composition, and higher weight percentage of SGO (> 0.5%) would decrease the activity of silver carbonate (SI: 4a, b).

Similar to methylene blue, other organic dyes like tartrazine, rhodamine B, methyl orange (Fig. 9), and pesticide thiram were degraded by this modified silver carbonate within a very short time. The spectra indicate the decrease in the absorption peak of organic pollutants. Thus, the efficiency of 0.5% SGO-Ag_2CO_3 photocatalyst is very high compared to pure silver carbonate.

The removal of organic contents from dyes was evaluated using TOC analysis (SI: 5). SGO-Ag_2CO_3 nanocomposite was more active for the degradation of cationic dyes like methylene blue and rhodamine B. The removal

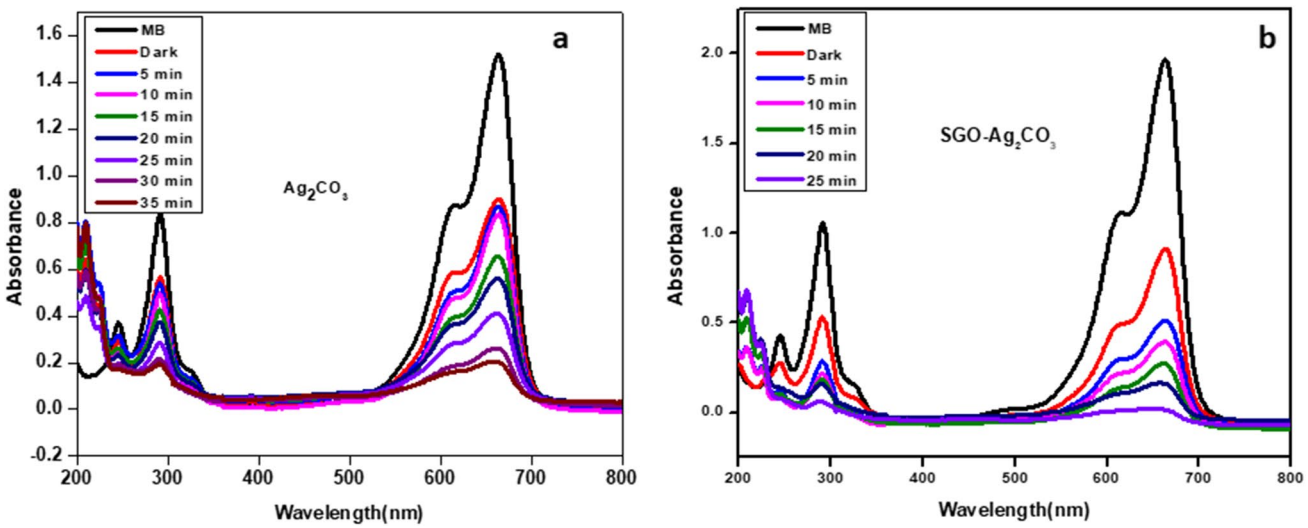

Fig. 8 Methylene blue degradation using **a** Ag_2CO_3, **b** SGO-Ag_2CO_3

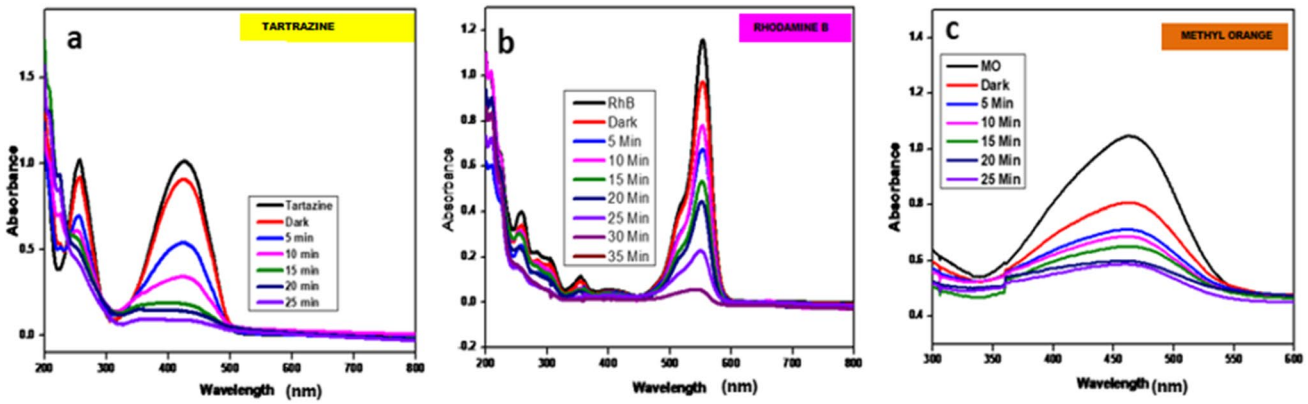

Fig. 9 Degradation of different dyes: **a** tartrazine, **b** Rh B, and **c** MO using 0.5% of SGO-Ag_2CO_3

of fungicide thiram was studied using HPLC analysis (Fig. 10). The pure thiram has sharp peak at a retention time of 4.7 min and a minor peak at 3.1 min. After 1 h of photodegradation, the sharp peak of thiram was completely removed. The degraded product of thiram was analyzed using mass spectrometry. The mass spectrum of pure thiram and degraded product after 2-h sunlight exposure were recorded. The mass spectrum of thiram shows a strong peak at m/z = 240.99 as the most intense peak, and after degradation, the peak at m/z = 240.99 was disappeared, and a new peak at m/z = 90.05 was formed. The expected degraded product from thiram with m/z = 90.054 is N-methylthiourea, which is less toxic than thiram (SI: 6a, b)(Fig. 11).

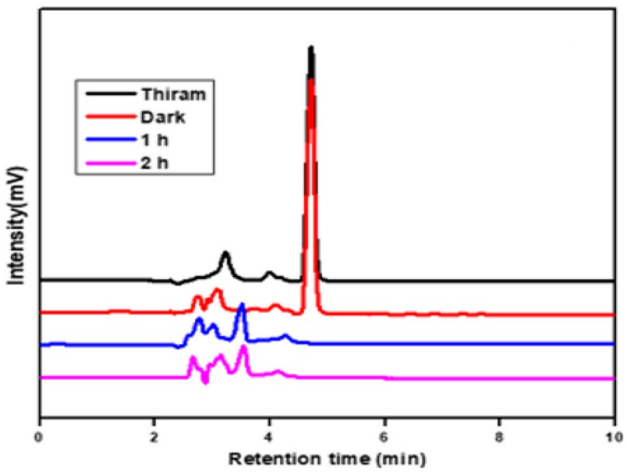

Fig. 10 HPLC chromatogram of thiram

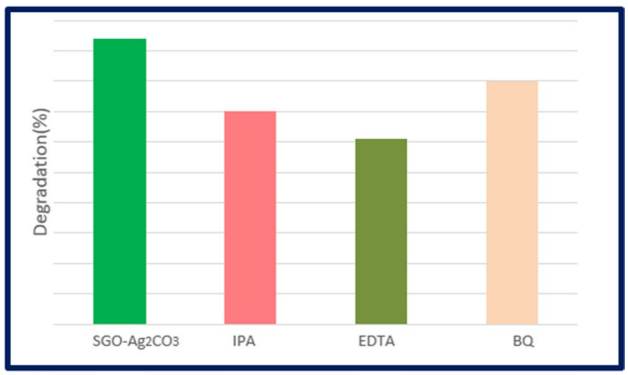

Fig. 11 Percentage degradation of methylene blue using different scavengers

Scavenger study

The photocatalysts upon irradiation by light produces charge carriers such as electrons and holes. Further, the electrons and hole upon reaction with oxygen and water in the catalytic system to produce superoxide and hydroxyl radical, respectively. These charge carriers are the real species converting pollutants to smaller fragments or simple CO_2 and H_2O. Hence, they are called the active species which determines the effect of catalysts. The amount of different active species varies from system to system. Hence, it is important to determine the presence and role of active species present in the photocatalytic system. To study the role of active species, chemicals are usually added to the system, which can capture and deactivate the active species and are called scavengers. Here, ethylenediaminetetra-acetic acid (EDTA), 1,4-benzoquinone, and isopropylalcohol were added as scavengers for holes, superoxide radicals, and hydroxyl radicals, respectively. The rate of degradation of MB was compared and found that the highest catalysis in the presence of IPA > EDTA > BQ indicates that the major active species responsible for the degradation is holes.

Stability of the catalyst

One of the important characteristics of a catalyst is its stability. The stability of the modified catalyst was studied using XRD analysis. Figure 12a shows the XRD spectrum of both fresh and used catalysts, and no appreciable change is observed in their spectrum. Similarly, the recyclability of the catalyst was studied by doing the photocatalytic degradation for four different cycles, and the plot of C/Co vs. time graph is given in Fig. 12b. From the first to the fourth cycle, the activity of the catalyst is almost the same, which supports the profounded stability of the fabricated composite catalyst.

Mechanism of photocatalytic degradation

Scheme 2 explains the mechanism of photodegradation using 0.5% SGO-Ag_2CO_3 as a photocatalyst. This photocatalyst is a binary heterojunction system. When the catalyst is irradiated with sunlight, the electrons in the valence band of Ag_2CO_3 are transferred to the conduction band leaving holes in the valence band. This creates e^-—h^+ pairs which are the charge carriers. The electrons in the conduction band of silver carbonate are transferred to the SGO sheet. Thus, the charge carriers can move throughout the system to keep the electrons and holes far away to avoid charge recombination

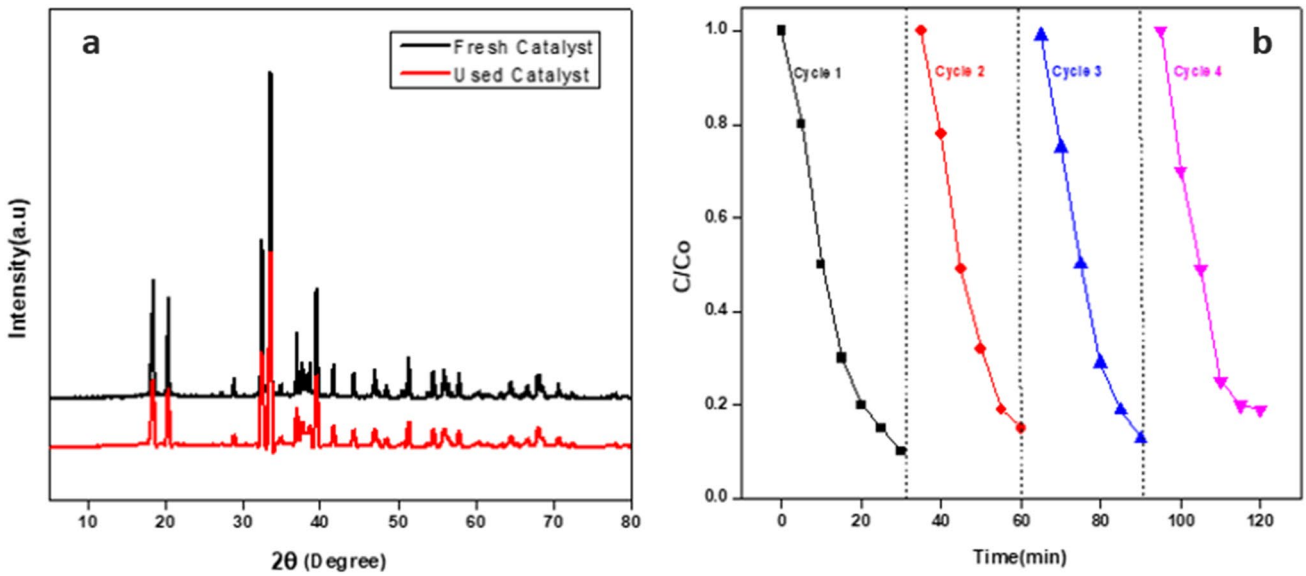

Fig. 12 **a** XRD spectra of fresh and used catalyst and **b** C/Co vs time graph of recycling study of SGO-Ag_2CO_3

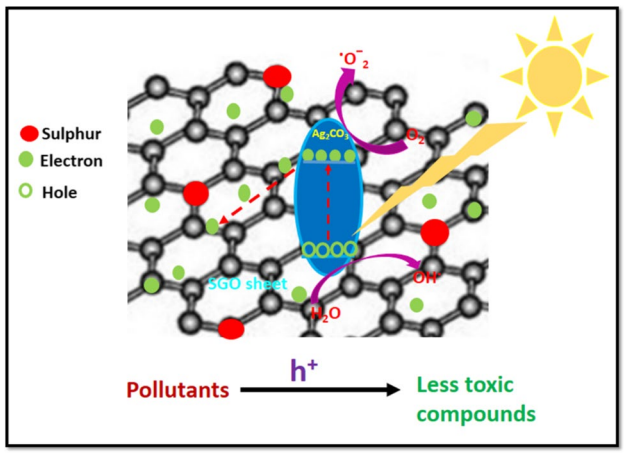

Scheme 2 Proposed mechanism of photocatalytic degradation by SGO-Ag_2CO_3

as revealed by the PL spectra. The high conductivity of sulfur-doped graphene oxide assists the separation between photo-generated electron–hole pairs and decreases the rate of charge carriers recombination. The free electron in the system is used for the conversion of surface O_2 molecules into superoxide radicals ($^{\cdot}O_2^-$). The conduction band potential of Ag_2CO_3 is found as 0.34 eV which is not sufficient for the generation of superoxide radicals from O_2 molecules adsorbed on the surface (E [$O_2/O_2^{\cdot-}$] is − 0.33 eV vs. NHE). The valence band potential of Ag_2CO_3 is 2.70 eV which is more positive than the potential essential for the generation of hydroxyl radicals from water (E [OH − /OH·] is 2.38 eV vs. NHE). But scavenger study showed that holes are the major active species of the system. The holes degrade organic pollutants to less toxic compounds and finally give CO_2 and water which are the by-products of this photocatalytic process.

$$Ag_2CO_3 + h\upsilon \rightarrow Ag_2CO_3(h^+) + Ag_2CO_3(e^-) \quad (6)$$

$$SGO + h\upsilon \rightarrow SGO(h^+) + SGO(e^-) \quad (7)$$

$$Ag_2CO_3(e^-)\text{or}SGO(e^-) \rightarrow {}^{\cdot}O_2^- + Ag_2CO_3\text{or}SGO \quad (8)$$

$$Ag_2CO_3(h^+)\text{or}SGO(h^+) \rightarrow OH^{\cdot} + Ag_2CO_3 + SGO \quad (9)$$

Conclusions

The novel SGO-Ag_2CO_3 photocatalyst was successfully synthesized by the simple precipitation method. The synthesized photocatalyst was characterized by XRD, IR, UV–vis DRS, PL, XPS, SEM, TEM, and electrochemical techniques. Short rod-shaped Ag_2CO_3 distributed all over the surface of SGO bestows efficient charge carrier transport. The 0.5% SGO-Ag_2CO_3 photocatalyst exhibited higher photocatalytic activity for MB, RhB, MO, tartrazine, and thiram degradation under visible light irradiation. The modification of Ag_2CO_3 using SGO resulted in a decrease in band gap compared to pure silver carbonate which is very favorable for the improvement in photocatalytic action. The SGO-Ag_2CO_3 shows higher light absorption and lower electron–hole pair recombination. The incorporation of SGO led to an increase in conductivity and photocurrent. From the scavenger study, holes were found to have major active species of degradation. A plausible mechanism for the degradation has been derived from different studies. The newly fabricated SGO-Ag_2CO_3 binary hetero structure will be applicable for the removal of organic pollutants from wastewater.

Supplementary Information The online version contains supplementary material available at https://doi.org/10.1007/s11356-022-19606-z.

Author contribution NJ contributed in the conceptualization, methodology, resources, and writing the original draft. RNP, TA, MSP, and BKJ participated in data curation and visualization. BM contributed in the conceptualization, supervision, project administration, and review and editing of manuscript. All the authors actively participated in the reading and approval of final manuscript.

Availability of data and materials Not applicable.

Declarations

Ethics approval and consent to participate Not applicable.

Consent for publication Not applicable.

Competing interests The authors declare no competing interests.

References

Abraham T, Priyanka RN, Joseph S, Plathanam NJ, M.G., G., & Mathew, B. (2020) Flower-like MoS_2/$BiFeO_3$ doped silver orthophosphate catalyst for visible-light assisted treatment of refractory organic pollutants. Appl Mater Today 21:100845. https://doi.org/10.1016/j.apmt.2020.100845

Arumugam Senthil R, Khan A, Pan J, Osman S, Yang V, Kumar TR, Liu X (2020) A facile single-pot synthesis of visible-light-driven AgBr/Ag_2CO_3 composite as efficient photocatalytic material for water purification. Colloids Surf, A Physicochem Eng Asp 586:124183. https://doi.org/10.1016/j.colsurfa.2019.124183

Arunpandian M, Selvakumar K, Raja A, Rajasekaran P, Thiruppathi M, Nagarajan ER, Arunachalam S (2019) Fabrication of novel Nd_2O_3/ZnO-GO nanocomposite: an efficient photocatalyst for the degradation of organic pollutants. Colloids Surf A Physicochem Eng Asp 567:213–227. https://doi.org/10.1016/j.colsurfa.2019.01.058

Asadollahi A, Sohrabnezhad S, Ansari R (2017) Enhancement of photocatalytic activity and stability of Ag2CO3 by formation of

AgBr/Ag_2CO_3 heterojunction in mordenite zeolite. Adv Powder Technol 28(1):304–313. https://doi.org/10.1016/j.apt.2016.10.004

Chen L, Hua H, Yang Q, Liu J, Han X, Li Y, Hu C (2018) Rational electron transmission structure in an Ag_2O/TiO_2 (anatase-B) system for effective enhancement of visible light photocatalyticactivity. J Phys Chem C 123(3):1817–1827. https://doi.org/10.1021/acs.jpcc.8b09783

Dai G, Yu J, Liu G (2012) A new approach for photocorrosion inhibition of Ag_2CO_3 photocatalyst with highly visible-light-responsive reactivity. J Phys Chem C 116(29):15519–15524. https://doi.org/10.1021/jp305669f

Dong S, Ding X, Guo T, Yue X, Han X, Sun J (2017) Self-assembled hollow sphere shaped Bi_2WO_6 /RGO composites for efficient sunlight-driven photocatalytic degradation of organic pollutants. Chem Eng J 316:778–789. https://doi.org/10.1016/j.cej.2017.02.017

Dostanić J, Lončarević D, Đorđević V, Ahrenkiel SP, Nedeljković JM (2017) The photocatalytic performance of silver halides – silver carbonate heterostructures. J Photochem Photobiol 336:1–7. https://doi.org/10.1016/j.jphotochem.2016.12.019

Feng M, Zhang M, Song J-M, Li X-G, Yu S-H (2011) Ultralong silver trimolybdate nanowires: synthesis, phase transformation, stability, and their photocatalytic, optical, and electrical properties. ACS Nano 5(8):6726–6735. https://doi.org/10.1021/nn202296h

Fu S, Yuan W, Yan Y, Liu H, Shi X, Zhao F, Zhou J (2019) Highly efficient visible-light photoactivity of Z-scheme MoS_2/Ag_2CO_3 photocatalysts for organic pollutants degradation and bacterial inactivation. J Environ Manage 252: 109654. coll

Han L, Xu Z, Wang P, Dong S (2013) Facile synthesis of a free-standing Ag@AgCl film for a high performance photocatalyst and photodetector. ChemComm 49(43):4953. https://doi.org/10.1039/c3cc41798k

Han W, Chen L, Song W, Wang S, Fan X, Li Y et al (2018) Synthesis ofnitrogen and sulfur co-doped reduced graphene oxide as efficient metal-free cocatalyst for the photo-activity enhancement of CdS. Appl Catal B Environ 236:212–221. https://doi.org/10.1016/j.apcatb.2018.05.021

Hu B, Wu L-H, Liu S-J, Yao H-B, Shi H-Y, Li G-P, Yu S-H (2010) Microwave-assisted synthesis of silver indium tungsten oxide mesocrystals and their selective photocatalytic properties. ChemComm 46(13):2277. https://doi.org/10.1039/b921455k

Hunge YM, Yadav AA, Mathe VL (2018) Ultrasound assisted synthesis of WO_3-ZnO nanocomposites for brilliant blue dye degradation. Ultrason Sonochem 45:116–122. https://doi.org/10.1016/j.ultsonch.2018.02.052

Joseph S, Abraham S, Abraham T, Priyanka RN, Mathew B (2019) S-rGO modified sulphur doped carbon nitride with mixed-dimensional hierarchical nanostructures of silver vanadate for the enhanced photocatalytic degradation of pollutants in divergent fields. Appl Surf Sci 495:143478. https://doi.org/10.1016/j.apsusc.2019.07.220

Khurram R, Wang Z, Ehsan MF (2021) α-Fe_2O_3-based nanocomposites: synthesis, characterization, and photocatalytic response towards wastewater treatment. Environ Sci Pollut Res 28(14):17697–17711. https://doi.org/10.1007/s11356-020-11778-w

Li F, Liu S, Qi R, Li H, Cui T (2017) Effective visualization of latent fingerprints with red fluorescent $La_2(MoO_4)_3:Eu^{3+}$ microcrystals. J Alloys Compd 727:919–924. https://doi.org/10.1016/j.jallcom.2017.08.182

Li J, Guan R, Zhang J, Zhao Z, Zhai H, Sun D, Qi Y (2019) Preparation and photocatalytic performance of dumbbell Ag_2CO_3–ZnO heterojunctions. ACS Omega 5(1):570–577. https://doi.org/10.1021/acsomega.9b03131

Li T, Hu X, Liu C, Tang C, Wang X, Luo S (2016) Efficient photocatalytic degradation of organic dyes and reaction mechanism with $Ag_2CO_3/Bi_2O_2CO_3$ photocatalyst under visible light irradiation.J. Mol Catal 425:124–135. https://doi.org/10.1016/j.molcata.2016.10.001

Li Y, Fang L, Jin R, Yang Y, Fang X, Xing Y, Song S (2015) Preparation and enhanced visible light photocatalytic activity of novel g-C_3N_4 nanosheets loaded with Ag_2CO_3 nanoparticles. Nanoscale 7(2):758–764. https://doi.org/10.1039/c4nr06565d

Liu H-Y, Liang C, Niu C-G, Huang D-W, Du Y-B, Guo H, Zeng G-M (2019) Facile assembly of g-C_3N_4/Ag_2CO_3/graphene oxide with a novel dual Z-scheme system for enhanced photocatalytic pollutant degradation. Appl Surf Sci 475:421–434. https://doi.org/10.1016/j.apsusc.2019.01.018

Liu L, Hu T, Dai K, Zhang J, Liang C (2021) A novel step-scheme $BiVO_4/Ag_3VO_4$ photocatalyst for enhanced photocatalytic degradation activity under visible light irradiation. Chinese J Catal 42(1):46–55. https://doi.org/10.1016/s1872-2067(20)63560-4

Liu W, Liu X, Fu Y, You Q, Huang R, Liu P, Li Z (2012) Nanocrystalline pyrochlore $AgSbO_3$: hydrothermal synthesis, photocatalytic activity and self-stable mechanism study. Appl Catal B 123–124:78–83. https://doi.org/10.1016/j.apcatb.2012.04.033

Liu Y, Kong J, Yuan J, Zhao W, Zhu X, Sun C, Xie J (2018) Enhanced photocatalytic activity over flower-like sphere Ag/$Ag_2CO_3/BiVO_4$ plasmonic heterojunction photocatalyst for tetracycline degradation. Chem Eng J 331:242–254. https://doi.org/10.1016/j.cej.2017.08.114

Longo E, Cavalcante LS, Volanti DP, Gouveia AF, Longo VM, Varela JA, Andrés J (2013) Direct in situ observation of the electron-driven synthesis of Ag filaments on α-Ag_2WO_4 crystals. Sci Rep 3(1). https://doi.org/10.1038/srep01676

Low J, Zhang L, Tong T, Shen B, Yu J (2018) TiO_2/MXene Ti_3C_2 composite with excellent photocatalytic CO_2 reduction activity. J Catal 361:255–266. https://doi.org/10.1016/j.jcat.2018.03.009

Petala A, Nasiou A, Mantzavinos D, Frontistis Z (2020) Photocatalytic evaluation of Ag_2CO_3 for ethylparaben degradation in different water matrices. Water 12(4):1180. https://doi.org/10.3390/w12041180

Pirhashemi M, Habibi-Yangjeh A (2018) Visible-light photosensitization of ZnO by Bi_2MoO_6 and AgBr: role of tandem n-n heterojunctions in efficient charge transfer and photocatalytic performances. Mater Chem Phys 214:107–119. https://doi.org/10.1016/j.matchemphys.2018.04.089

Pirzada BM, Pushpendra, Kunchala RK, Naidu BS (2019) Synthesis of $LaFeO_3/Ag_2CO_3$ nanocomposites for photocatalytic degradation of rhodamine b and p-chlorophenol under natural sunlight. ACS Omega, 4(2), 2618–2629. https://doi.org/10.1021/acsomega.8b02829

Priyanka RN, Abraham T, Joseph S, George JM, Plathanam NJ, Mathew B (2021) Fast and efficient degradation of water pollutant dyes and fungicide by novel sulfur-doped graphene oxide–modified Ag_3PO_4 nanocomposite. Environ Sci Pollut Res 28(16):20247–20260. https://doi.org/10.1007/s11356-020-11884-9

Priyanka RN, Joseph S, Abraham T, Plathanam NJ, Mathew B (2020) Rapid sunlight-driven mineralisation of dyes and fungicide in water by novel sulphur-doped graphene oxide/Ag_3VO_4 nanocomposite. Environ Sci Pollut Res 27(9):9604–9618. https://doi.org/10.1007/s11356-019-07569-7

Safajou H, Khojasteh H, Salavati-Niasari M, Mortazavi-Derazkola S (2017) Enhanced photocatalytic degradation of dyes over graphene/Pd/TiO_2 nanocomposites: TiO_2 nanowires versus TiO_2 nanoparticles. J Colloid Interface Sci 498:423–432. https://doi.org/10.1016/j.jcis.2017.03.078

Song S, Meng A, Jiang S, Cheng B, Jiang C (2017) Construction of Z-scheme Ag_2CO_3/N-doped graphene photocatalysts with enhanced visible-light photocatalytic activity by tuning the nitrogen species. Appl Surf Sci 396:1368–1374. https://doi.org/10.1016/j.apsusc.2016.11.168

Tang J, Liu Y, Li H, Tan Z, Li D (2013) A novel Ag_3AsO_4 visible-light-responsive photocatalyst: facile synthesis and exceptional photocatalytic performance. ChemComm 49(48):5498. https://doi.org/10.1039/c3cc41090k

Tian Z, Li J, Zhu G, Lu J, Wang Y, Shi Z, Xu C (2016) Facile synthesis of highly conductive sulfur-doped reduced graphene oxide sheets. Phys Chem Chem Phys 18(2):1125–1130. https://doi.org/10.1039/c5cp05475c

Tonda S, Kumar S, Shanker V (2015) In situ growth strategy for highly efficient Ag_2CO_3/g-C_3N_4 hetero/nanojunctions with enhanced photocatalytic activity under sunlight irradiation. J Environ Chem Eng 3(2):852–861. https://doi.org/10.1016/j.jece.2015.03.021

Wang C, Yan J, Wu X, Song Y, Cai G, Xu H, Li H (2013) Synthesis and characterization of AgBr/$AgNbO_3$ composite with enhanced visible-light photocatalytic activity. Appl Surf Sci 273:159–166. https://doi.org/10.1016/j.apsusc.2013.02.004

Wang S, Li D, Sun C, Yang S, Guan Y, He H (2014a) Synthesis and characterization of g-C_3N_4/Ag_3VO_4 composites with significantly enhanced visible-light photocatalytic activity for triphenylmethane dye degradation. Appl Catal B 144:885–892. https://doi.org/10.1016/j.apcatb.2013.08.008

Wang W, Liu Y, Zhang H, Qian Y, Guo Z (2017) Re-investigation on reduced graphene oxide/Ag_2CO_3 composite photocatalyst: an insight into the double-edged sword role of RGO. Appl Surf Sci 396:102–109. https://doi.org/10.1016/j.apsusc.2016.11.030

Wang X, Zhan S, Wang Y, Wang P, Yu H, Yu J, Hu C (2014b) Facile synthesis and enhanced visible-light photocatalytic activity of Ag_2S nanocrystal-sensitized $Ag_8W_4O_{16}$ nanorods. J Colloid Interface Sci 422:30–37. https://doi.org/10.1016/j.jcis.2014.02.009

Wang Y, Ren P, Feng C, Zheng X, Wang Z, Li D (2014c) Photocatalytic behavior and photo-corrosion of visible-light-active silver carbonate/titanium dioxide. Mater Lett 115:85–88. https://doi.org/10.1016/j.matlet.2013.10.025

Wen X-J, Niu C-G, Guo H, Zhang L, Liang C, Zeng G-M (2018) Photocatalytic degradation of levofloxacin by ternary Ag_2CO_3/CeO_2/AgBr photocatalyst under visible-light irradiation: degradation pathways, mineralization ability, and an accelerated interfacial charge transfer process study. J Catal 358:211–223. https://doi.org/10.1016/j.jcat.2017.12.005

Wu X, Hu Y, Wang Y, Zhou Y, Han Z, Jin X, Chen G (2019) In-situ synthesis of Z-scheme Ag2CO3/Ag/AgNCO heterojunction photocatalyst with enhanced stability and photocatalytic activity. Appl Surf Sci 464:108–114. https://doi.org/10.1016/j.apsusc.2018.09.059

Xie J, Fang C, Zou J, Lu H, Tian C, Han C, Zhao D (2016) In situ ultrasonic formation of AgBr/Ag_2CO_3 nanosheets composite with enhanced visible-driven photocatalytic performance. Mater Lett 170:62–66. https://doi.org/10.1016/j.matlet.2016.02.002

Xu C, Liu Y, Huang B, Li H, Qin X, Zhang X, Dai Y (2011) Preparation, characterization, and photocatalytic properties of silver carbonate. Appl Surf Sci 257(20):8732–8736. https://doi.org/10.1016/j.apsusc.2011.05.060

Xu D, Cheng B, Cao S, Yu J (2015a) Enhanced photocatalytic activity and stability of Z-scheme Ag_2CrO_4-GO composite photocatalysts for organic pollutant degradation. Appl Catal B 164:380–388. https://doi.org/10.1016/j.apcatb.2014.09.051

Xu D, Cheng B, Zhang J, Wang W, Yu J, Ho W (2015b) Photocatalytic activity of Ag_2MO_4 (M = Cr, Mo, W) photocatalysts. J Mater Chem a 3(40):20153–20166. https://doi.org/10.1039/c5ta05248c

Xu H, Song Y, Song Y, Zhu J, Zhu T, Liu C, Li H (2014) Synthesis and characterization of g-C_3N_4/$Ag_2CO_3$with enhanced visible-light photocatalytic activity for the degradation of organic pollutants. RSC Adv 4(65):34539. https://doi.org/10.1039/c4ra03443k

Yi Z, Ye J, Kikugawa N, Kako T, Ouyang S, Stuart-Williams H, Withers RL (2010) An orthophosphate semiconductor with photooxidation properties under visible-light irradiation. Nat Mater 9(7):559–564. https://doi.org/10.1038/nmat2780

Yu C, Wei L, Zhou W, Dionysiou DD, Zhu L, Shu Q, Liu H (2016) A visible-light-driven core-shell like Ag_2S@Ag_2CO_3 composite photocatalyst with high performance in pollutants degradation. Chemosphere 157:250–261. https://doi.org/10.1016/j.chemosphere.2016.05.021

Zhu X, Qiu F, Li X, Rong X, Wang J, Yang D (2016) Silver carbonate loaded on activated carbon composite photocatalyst with enhanced photocatalytic activity under visible light irradiation. Mater Technol 32(1):38–45. https://doi.org/10.1080/10667857.2015.1116219